

## Density Functional Theory Study of the Reaction Behavior Histidine Modified Polyamidoamine Dendrimer as Nanocarrier for Delivery of Ectoine Drug

N. Madadi Mahani<sup>a,\*</sup>, F. Mostaghni and H. Shafiekhani

*Department of Chemistry, Payame Noor University, 19395-4697, Tehran, Iran*

*(Received 27 June 2021, Accepted 23 October 2021)*

In the present paper, the complexation of Ectoine drugs with pristine PAMAM and Histidine modified PAMAM dendrimers was investigated by density functional theory. The bond between Ectoine and PAMAM dendrimers was established via a cross-linking agent, EDC/NHS, which is associated with the formation of amides bond between the two species. The results of the modeling were obtained by B3LYP/6-311G approach for all forms of the PAMAM-drug complexes. Due to the results, the complex of ectoine-histidine modified PAMAM dendrimer turns to absorb more electrons than ectoine-PAMAM dendrimer in a water solvent. Furthermore, the topological analysis and the electron localization function show that the nature of the bond is purely covalent and their bond order is one in both phases. DOS plots of drug-dendrimers are similar to the trends of their energy gaps in two phases. In addition, the binding energy between Ectoine drug and dendrimers showed that this energy decreases from gas phase to solvent phase. The complex has displayed a meaningful improvement of electronic and structural properties. Therefore, it represented that both PAMAM dendrimers being combined with the Ectoine drug are appropriate for use in drug delivery.

**Keywords:** Computational investigation, Drug delivery, Cross-linking, Natural bond orbital analysis, Topological analysis

### INTRODUCTION

In the present century, one of the most serious and common diseases is cancer. Using the nanocarriers of anticancer drugs like liposomes, micelles, solid lipid nanoparticles, polymeric nanoparticles, nanocages, carbon nanotubes, nanocrystals, graphene oxide, gold nanoparticles, and dendrimers indicated an appropriate therapy for cancer by targeting tumor cells without side effects on other cells [1-8]. The considerable monodisperse structure of dendrimers gives its specific characteristics like solubility, reactivity, penetration, well-defined tunable nanosize range, degree of uniformity, structure, globular morphology, capabilities to pass via cell walls owing to their controllable size and lipophilicity, excellent flexibility, and functional performance [9-10]. Due to these characteristics, they are an appropriate vehicle to transfer

the genes and drugs [11]. Dendrimers serve as carriers for various anticancer drugs like 5-fluorouracil [12], cisplatin [13], doxorubicin [14], paclitaxel [15], 10-hydroxycamptothecin [16] and melphalan [17].

Polyamidoamines dendrimers with greatly special and hierarchical three-dimensional architecture, are one of the dendrimers which are highly utilized as proper carriers to deliver drugs and tissue engineering and regenerative medicine [18,19]. Wu *et al.* were reported that the histidine modified PAMAM dendritic can be applied as efficient chemotherapeutic drug vehicles in cancer treatment [20]. The reactions of drug-dendrimer are so significant in pharmaceutical industry, the biomedical sciences and pharmaceutical industry. Surveying these reactions can help develop chemistry in biomedical and pharmaceutical science [21]. Ectoine drug is considered as one natural metabolite that forces the apoptosis in the cells of lung cancer [22]. It could be applied as a medicine for the treatment of lung cancer after more optimization of

\*Corresponding author. E-mail: nmmadady@gmail.com

formulations or as an auxiliary drug. Since it has no toxic impact on other cells [23, 24].

An approach for cross-linking and immobilization of NH<sub>2</sub>-containing biomolecules onto carboxyl-containing compounds through covalent amide bond is using N-ethyl-N<sup>0</sup>-(3-(dimethylamino) propyl) carbodiimide (EDC) and N-hydroxysuccinimide (NHS) [25,26]. Sam et al. investigated in situ EDC/NHS activation of end carboxylic acids of an undecylenic acid (UA) monolayer on porous silicon [27].

In the present study, the bonding of PAMAM and histidine modified PAMAM with Ectoine drug was theoretically investigated. The bond between Ectoine and dendrimers was established through a cross-linking agent, 1-ethyl-3-(3-dimethylaminopropyl)-carbodiimide/N-hydroxysuccinimide that is correlated to the formation of amides bond between drug and dendrimer. This study aims to access the information about electronic characteristics, chemical bond nature due to the topological analysis of electron density, the natural electronic configurations by natural bond orbital analysis, and the bond order analysis due to the Laplacian electron density of the reaction of PAMAM and histidine modified PAMAM and Ectoine applying DFT computational method.

A numbers of researchers were utilized PAMAM in theoretical computations. The adsorption of 5 fluorouracil drug on PAMAM carriers has been surveyed with M06-2X and B3LYP functional in an aqueous solution [28]. A theoretical study of the structural probabilities of nanostructure complex formation between polyamidoamine dendrimers and some drugs which suppress hepatitis virus growth has been handled with RHF/PM6 approach [29]. The interaction between PAMAM dendrimer and Tran's isomer of Picoplatin anticancer drug has been studied by DFT [30]. A theoretical study on the reactivity and the structural properties of the Melphalan anticancer drug with PAMAM dendrimer has been done in both phases of gas and solvent [31].

Also, the interaction between PAMAM G0 and gold nanoclusters has been studied theoretically at DFT level [32]. Further computational study of amine-and acetyl-terminated PAMAM-dexamethasone 21-phosphate complexation has been performed for atomic-level characterization of dendrimer-drug complexes [33]. The use of theoretical and computational methods to evaluate the

loading of the drug in the PAMAM carrier and its release process in the target area has advantages over experimental methods [34-36]. Besides, the theoretical design of dendrimeric fractal patterns for the encapsulation of salicylanilides drug has been investigated [37].

Our study's results can help a better viewpoint of the reaction between PAMAM and histidine modified PAMAM with Ectoine and proper information about bonding of the reaction between PAMAM and histidine modified PAMAM with Ectoine.

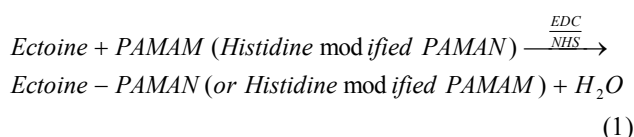
## COMPUTATIONAL METHODS

All geometrical optimizations and quantum chemical calculations of Ectoine, PAMAM, histidine modified PAMAM, and their complexes were performed using Gaussian 09 program [38] by Becke's three-parameter Lee-Yang-Parr hybrid functional (B3LYP) [39] with 6-311G basis set in the solution and gas phases. DFT computations present us with excellent viewpoints into structural geometry changes, interaction energy, and load distribution in the encapsulation process. Frequency computations are done to remove the imaginary frequencies and gain minimum energy. Quantum Theory of Atoms in Molecules and Multifunctional Wavefunction Analyzer [40] are applied to investigate the nature of interaction and binding among the atoms of PAMAM and ectoine by the topological analysis of the electron densities. Moreover, Fuzzy bond order [41], Mayer bond order [42], and natural bond orbital (NBO) for PAMAM-Ectoine and histidine modified PAMAM-Ectoine were calculated.

Besides, the function of electron localization as a measurement of the likelihood of finding an electron in the neighborhood space of a reference electron located at a given point and with the same spin [43] was achieved by Multiwfn code. For simulating the biological system, configurations are surveyed in the solvent phase. Surveying solvent impacts was done using the integral equation formalism polarized continuum model of self-consistent reaction field [44]. The descriptors of quantum chemical as an energy gap, and electronegativity and global hardness can be used to assess the chemical reactivity which is computed. The bond between ectoine with PAMAM and histidine modified PAMAM is made by a cross-linking

applying EDC-NHS.

The final reaction between the drug and PAMAM (histidine modified PAMAM) can be written as follows:



The bonding energies resulting from the reaction between the Ectoine molecule and the PAMAM (histidine modified PAMAM) can be acquired from Eq. (2).

$$\Delta X_{\text{binding}} = X_{\text{complex}} + X_{\text{H}_2\text{O}} - X_{\text{Ectoine}} + X_{\text{(PAMAM (Histidine modified PAMAM))}} \quad (2)$$

Where X is the enthalpy (H), the Gibbs free energy (G) or total energy (E), and  $X_{\text{complex}}$  is correspond to the values of the PAMAM-Ectoine or histidine modified PAMAM-Ectoine.

## RESULTS AND DISCUSSION

We have firstly optimized the structures of PAMAM, dendrimer, histidine modified PAMAM, and Ectoine in gas and solvent phases. The structures of PAMAM dendrimer and Ectoine were shown in Fig. 1. Moreover, the optimized configurations of histidine modified PAMAM G0, PAMAM- Ectoine, and histidine modified PAMAM-Ectoine in the solvent phase were indicated in Fig. 2.

The chemical reactivity descriptors of Ectoine, PAMAM, and Histidine modified PAMAM, PAMAM-Ectoine and Histidine modified PAMAM-Ectoine have shown in Table 1. The global hardness and energy gap of Ectoine in the solvent phase is less than the gas phase. Therefore, ectoine stability is less in the water solvent and its reactivity is higher. The global hardness and energy gap of PAMAM and Histidine modified PAMAM in the solvent phase is greater than the gas phase.

Table1 indicates gap energy, global hardness, and electronegativity of histidine modified PAMAM is greater than pristine PAMAM. Thus, the reactivity of Histidine modified PAMAM in the solvent phase is higher. After binding, the energy gap and global hardness of PAMAM-

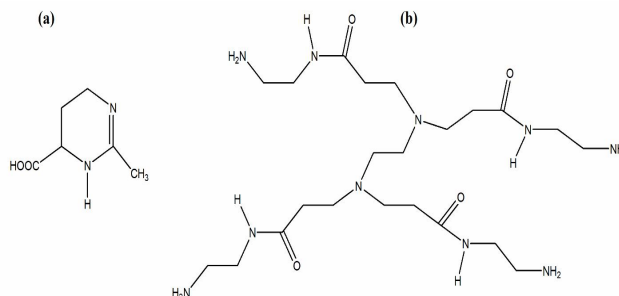


**Fig. 1.** The structures of the Ectoine (a) and PAMAM (b).

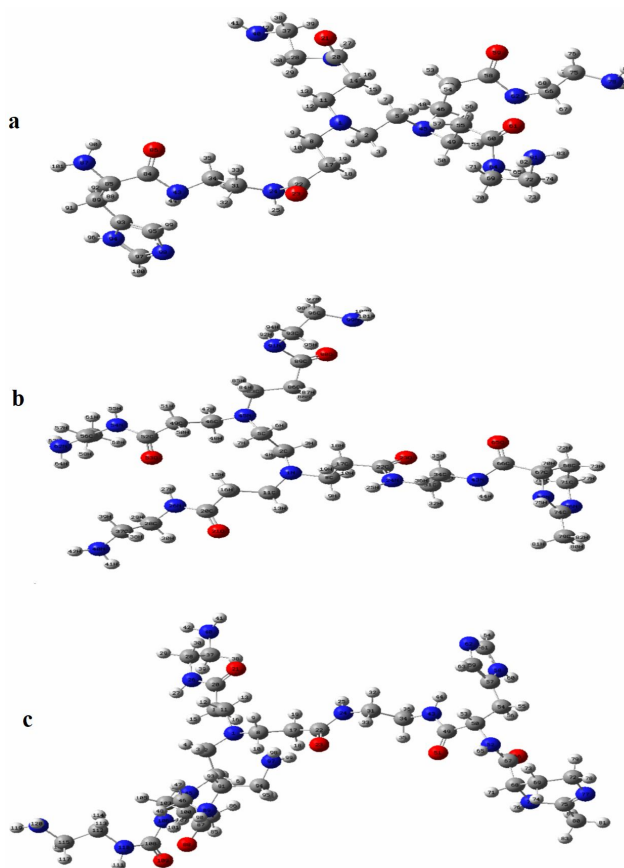


**Fig. 2.** The optimized configurations of the histidine modified PAMAM (a), PAMAM-Ect (b), and histidine modified PAMAM-Ect at solvent phase (c).

Ectoine complex decreased compared to free state ectoine in both phases and the energy gap increased compared to

**Table 1.** The Gap Energy, Global Hardness, and Electronegativity (eV) for PAMAM-Ect and PAMAM-His-Ect

Complex	$E_g = E_{LUMO} - E_{HOMO}$		$X = -(E_{HOMO} + E_{LUMO})/2$		$\eta = E_g/2$	
	Gas	Solvent	Gas	Solvent	Gas	Solvent
Ectoine	6.3037	6.0569	3.7614	3.7305	3.1518	3.0284
PAMAM	5.2629	5.2629	2.7487	2.8410	2.6314	2.7253
PAMAM-His	4.6221	5.2490	2.6571	2.9336	2.3110	2.6245
PAMAM-Ect	5.1927	5.4439	2.8127	2.8384	2.5963	2.7219
PAMAM-His-Ect	5.3650	5.4384	2.6180	2.7010	2.6825	2.71923

**Table 2.** The Binding, the Enthalpy, the Gibbs Free Energies, and Dipole Moment for PAMAM-Ect and PAMAM-His-Ect

Energies and dipole moment	PAMAM-Ect		PAMAM-His-Ect	
	Gas	Solvent	Gas	Solvent
$\Delta E$ (kJ mol <sup>-1</sup> )	-31.0851	-65.8344	-39.5844	-95.9344
$\Delta G$ (kJ mol <sup>-1</sup> )	-26.6251	-41.9948	-37.1875	-87.6746
$\Delta H$ (kJ mol <sup>-1</sup> )	-31.3983	-66.8163	-40.3526	-96.3558
$\mu$ (Debye)	7.5203	9.5619	9.7127	12.8765

PAMAM in a water solvent.

By surveying the electronegativity, it can be understood that PAMAM-Ectoine and Histidine modified PAMAM turn to absorb more electrons than the gas phase. Therefore, the reaction of Ectoine with PAMAM and histidine modified PAMAM causes a reduction in the electronegativity and reduced their energy gap and global hardness in both phases, but the amount of decrease is less in Histidine modified PAMAM. The reaction energies of Ectoine-PAMAM and Ectoine-Histidine modified PAMAM in both phases which are indicated in Table 2.

In both Ectoine -PAMAM and Ectoine-Histidine modified PAMAM systems, Gibbs free energies are negative which show the adsorption is spontaneous. Moreover, the negative enthalpies indicated that this reaction is exothermic. By comparing the binding, the enthalpy, and the Gibbs free energies for PAMAM-Ect and PAMAM-His-Ect, it can be concluded that the PAMAM-His-Ect complex is more stable. Furthermore, the polarity of molecules is shown by dipole moment. The polarity of PAMAM-Ect and PAMAM-His-Ect is higher in water solvent than in the gas phase and PAMAM-His-Ect complex is greater than PAMAM-Ect.

The saddle point on distributing electron density is

named bond critical point which has the electron density gradient of zero. BCP is characterized by the major diameter elements of the Hessian matrix of electron density. The whole three diameter elements of the Hessian matrix of electron density at a point is the Laplacian of electron density at that point [45]. The positive Laplacian shows the decrease in electrons and the negative Laplacian is related to many electrons.

At BCP, quantities as the Laplacian,  $\nabla^2\rho(r)$ , the potential energy density,  $V(r)$ , the positive definite kinetic energy density,  $G(r)$ , and the total electronic energy density,  $H(r) = V(r) + G(r)$ , in terms of which the bond degree,  $H(r)/\rho(r)$ , can be deliberated. In addition, Eq. (3), displays a helpful relationship between them:

$$\frac{1}{4}\nabla^2\rho(r) = V(r) + 2G(r) = H(r) + G(r) \quad (3)$$

The nature of chemical bonds could be distinguished by the values of potential and kinetic energy. The characteristics of chemical bonds can be shown by the amounts of potential and kinetic energy. The chemical bonds is covalent in case Laplacian and  $H(r)$  be negative,  $\rho(r) > 0.02$ ,  $G(r)/\rho(r)$  and  $G(r)/V(r) < 1$  [46]. Ionic interactions displays positive

**Table 3.** Electron Density Descriptors (a.u.) at the Bond Critical Points (BCP) between Atoms of Ectoine-PAMAM Complex

Atoms		$\rho(r)$	$\nabla^2\rho(r)$	Ellipticity	$-G(r)/V(r)$	$G(r)/\rho(r)$	$E(r)$
N <sub>43</sub> -H <sub>44</sub>	Gas	0.3224	-1.3125	0.0443	0.1274	0.1740	-0.3842
	Solvent	0.3224	-1.3049	0.0444	0.0128	0.0174	-0.4330
N <sub>69</sub> -H <sub>75</sub>	Gas	0.3235	-1.2446	0.0517	0.1381	0.1836	-0.3705
	Solvent	0.3235	-1.2442	0.0525	1.3860	1.8434	0.1661
N <sub>43</sub> -C <sub>66</sub>	Gas	0.3016	-0.7230	0.0785	0.03253	0.0558	-0.5004
	Solvent	0.3070	-0.7512	0.0717	0.3276	0.5817	-0.3665
O <sub>65</sub> -C <sub>66</sub>	Gas	0.3659	-0.73440	0.0208	0.3999	1.0029	-0.5507
	Solvent	0.3592	-0.7657	0.0249	0.3898	0.9434	-0.5304
C <sub>66</sub> -C <sub>67</sub>	Gas	0.2300	-0.39341	0.0776	0.2786	0.2689	-0.1601
	Solvent	0.2299	-0.3934	0.07819	2.7851	2.6888	0.3963
C <sub>67</sub> -C <sub>68</sub>	Gas	0.2203	-0.36879	0.0211	0.2796	0.2655	-0.1506
	Solvent	0.2212	-0.3732	0.0205	2.7885	2.6582	0.3772
C <sub>67</sub> -N <sub>69</sub>	Gas	0.2361	-0.4369	0.0410	0.3298	0.4483	-0.2152
	Solvent	0.2379	-0.4460	0.0393	0.3304	0.4568	-0.2202
C <sub>34</sub> -N <sub>43</sub>	Gas	0.2381	-0.4545	0.0128	0.33640	0.4905	-0.2304
	Solvent	0.2372	-0.4507	0.01154	0.3365	0.4893	-0.2289

**Table 4.** Electron Density Descriptors (a.u.) at the Bond Critical Points (BCP) between Atoms of Ectoine-Histidine Modified PAMAM Complex

Atoms		$\rho(r)$	$\nabla^2\rho(r)$	Ellipticity	$-G(r)/V(r)$	$G(r)/\rho(r)$	$E(r)$
C <sub>50</sub> -N <sub>52</sub>	Gas	0.2418	-0.4685	0.0355	0.3226	0.4399	-0.2234
	Solvent	0.2417	-0.4695	0.0368	0.3225	0.4414	-0.2241
N <sub>52</sub> -C <sub>67</sub>	Gas	0.2938	-0.6946	0.0646	0.3207	0.5288	-0.3291
	Solvent	0.2991	-0.7191	0.0600	0.3280	0.5733	-0.3513
N <sub>52</sub> -H <sub>65</sub>	Gas	0.3247	-1.2809	0.0475	1.3176	1.764039	0.1381
	Solvent	0.3244	-1.2767	0.0493	0.1324	0.177277	-0.37669
O <sub>66</sub> -C <sub>67</sub>	Gas	0.3676	-0.6921	0.0208	0.4083	1.0475	-0.558
	Solvent	0.3623	-0.7376	0.0269	0.3972	0.9842	-0.5412
C <sub>67</sub> -C <sub>68</sub>	Gas	0.2285	-0.3841	0.0702	2.8340	2.7505	0.4068
	Solvent	0.3624	-0.7376	0.0269	0.3972	0.9842	-0.5412
C <sub>68</sub> -C <sub>69</sub>	Gas	0.2189	-0.3639	0.0231	2.7927	2.6276	0.3693
	Solvent	0.2185	-0.3619	0.02058	2.8007	2.6365	0.3704
C <sub>68</sub> -N <sub>70</sub>	Gas	0.2495	-0.4984	0.0454	0.3174	0.434018	-0.2329
	Solvent	0.2464	-0.4841	0.0426	0.3191	0.4334	-0.2279
N <sub>70</sub> -H <sub>76</sub>	Gas	0.3248	-1.2843	0.0523	1.3244	1.7803	0.1417
	Solvent	0.3246	-1.2754	0.0543	1.3462	1.7979	0.1501

Laplacian and  $H(r)$ ,  $\rho(r) < 0.1$ ,  $G(r)/\rho(r)$  and  $G(r)/V(r) > 1$ .  
Electron density descriptors at the bond critical points for

the significant chemical bonds of PAMAM-Ect and PAMAM-His-Ect are shown in Table 3 and Table 4,

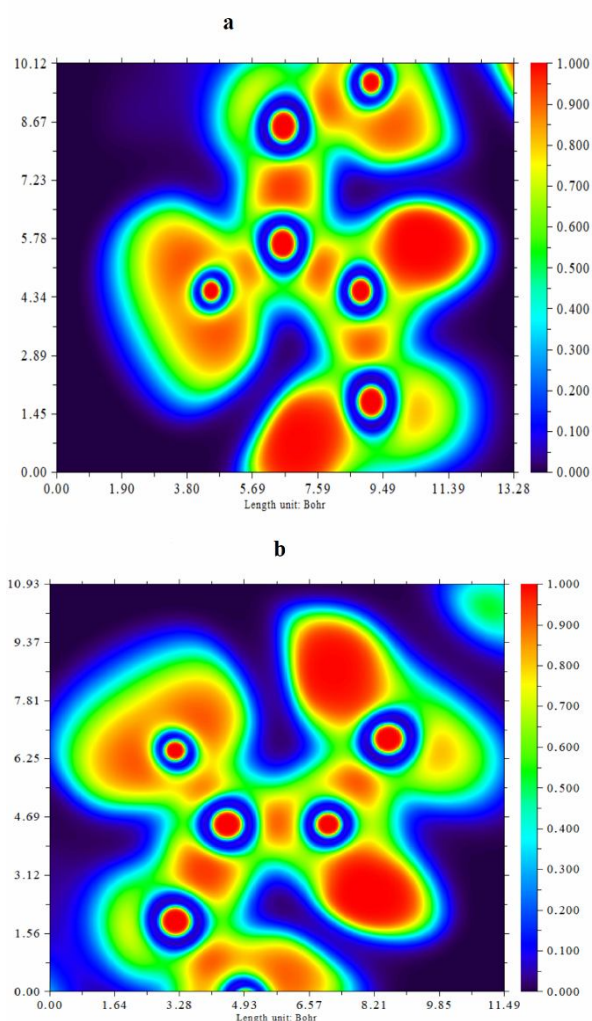


**Fig. 3.** ELF plots of optimized Ectoine-PAMAM a) at gas and b) at solvent phases.

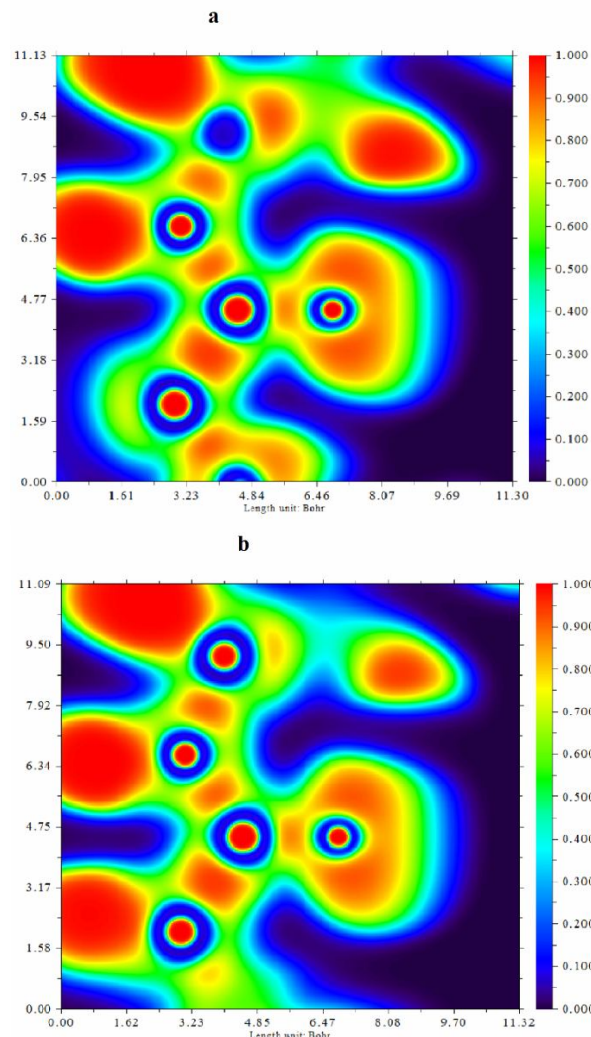


**Fig. 4.** ELF plots of optimized Ectoine-Histidine modified PAMAM a) at gas and b) at solvent phases.

respectively. Laplacian and  $E(r)$  of bonds are negative in gas and solvent phases. Moreover, the electron density values of them are higher than 0.02. The analysis of quantities as  $-G(r)/V(r)$ ,  $E(r)$ , and  $\rho(r)$  showed that these bonds are covalent kinds.

Analyzing the function of electron localization was done to corroborate the characteristics of bonds. ELF is an easy measurement of electron localization in atomic and molecular systems. ELF analysis can give information about the binding, the location of bonds, the electron pairs, the atomic structure of the system, and the strength of bond by integrating the electron density of the ELF area. To prove

the covalent bonding, ELF can be utilized [47]. ELF amount is between zero and one. By enhancing the ELF, the electrons become more localized and conceptualized, the characteristics of the atomic bond between two atoms gradually transform into covalent kind. ELF amounts are in the range from 0 to 1. By increasing the ELF, the characteristics of the bond become covalent kind due to the electrons becoming more concentrated and localized [48]. The topographical analysis of ELF of PAMAM-Ect and PAMAM-His-Ect are done which are indicated in Figs. 3 and 4, respectively, in both phases. The upper limit  $ELF = 1$  corresponds to perfect localization and the value  $ELF = \frac{1}{2}$

corresponds to electron-gas-like pair probability. ELF for the bond between reaction PAMAM-Ect and PAMAM-His-Ect are almost 0.45. The ELF analysis characterized N-C bonds are partly covalent that approved electron density analysis. Analyzing the natural bond orbitals prepare the electronic density distribution on atoms and bonds which is a beneficent instrument to understand the delocalization of electron density.

Tables 5 and 6 indicate NBO analysis after and before the reaction of Ectoine with PAMAM and histidine modified PAMAM for main atoms in both phases. Table 5 data show that the electron densities of orbitals have changed. The electron density of 2S and 2P orbitals of N43 was reduced in both phases after the reaction of Ectoine with PAMAM. For O84 atom, the electron density of 2s orbital increased after adsorption, while the electron density of 2P orbital was reduced in the gas phase. The electron density of 2S and 2P orbitals increased after the reaction in

the water solvent. For C85 atom, the electron density of 2P orbital of C85 in both phases increased after the reaction but the electron density of 2S orbital increased in the gas phase and do not alter in the solvent phase. For C87 atom, the electron densities of 2s and 2p orbitals in both phases have reduced. After the reaction, the electron densities of 1s orbitals of H44 atom have reduced by 0.07 and 0.06 in gas and solution phases, respectively. Moreover, the table indicates NBO analysis after and before the reaction of Ectoine with histidine modified PAMAM, Table 6 data indicates that the electron densities of N52 orbital after the reaction not have changed. For O66 and C67 atoms, the electron density of 2P orbital reduced and the electron density of 2S orbital increased after reaction in the gas phase. The electron density of 2P orbital increased in the water solvent.

The advancements of Wiberg bond order can be as Mayer and fuzzy bond order that have confirmed extremely

**Table 5.** The Natural Electron Configuration of some Atoms of the Ectoine before and after Reaction with PAMAM in Gas and Solvent Phases

Atoms	Gas		Solvent	
	Before	After	Before	After
N <sub>43</sub>	2S <sup>(1.41)</sup> 2p <sup>(4.41)</sup> 3p <sup>(0.01)</sup>	2S <sup>(1.32)</sup> 2p <sup>(4.37)</sup> 3p <sup>(0.01)</sup>	2S <sup>(1.42)</sup> 2p <sup>(4.45)</sup> 3p <sup>(0.01)</sup>	2S <sup>(1.26)</sup> 2p <sup>(4.33)</sup> 3p <sup>(0.01)</sup>
H <sub>44</sub>	1S <sup>(0.66)</sup>	1S <sup>(0.59)</sup>	1S <sup>(0.64)</sup>	1S <sup>(0.58)</sup>
C <sub>34</sub>	2S <sup>(1.00)</sup> 2p <sup>(3.16)</sup> 3p <sup>(0.01)</sup>	2S <sup>(1.01)</sup> 2p <sup>(3.16)</sup> 3p <sup>(0.01)</sup>	2S <sup>(1.00)</sup> 2p <sup>(3.16)</sup> 3s <sup>(0.01)</sup> 3p <sup>(0.01)</sup>	2S <sup>(1.01)</sup> 2p <sup>(3.17)</sup> 3p <sup>(0.01)</sup>
O <sub>84</sub>	2S <sup>(1.71)</sup> 2p <sup>(4.84)</sup>	2S <sup>(1.73)</sup> 2p <sup>(4.83)</sup>	2S <sup>(1.70)</sup> 2p <sup>(4.91)</sup>	2S <sup>(1.72)</sup> 2p <sup>(4.98)</sup>
C <sub>85</sub>	2S <sup>(0.76)</sup> 2p <sup>(2.44)</sup> 3s <sup>(0.01)</sup>	2S <sup>(0.77)</sup> 2p <sup>(2.53)</sup> 3s <sup>(0.01)</sup>	2S <sup>(0.77)</sup> 2p <sup>(2.41)</sup> 3s <sup>(0.01)</sup> 3p <sup>(0.03)</sup>	2S <sup>(0.77)</sup> 2p <sup>(2.53)</sup> 3s <sup>(0.01)</sup>
C <sub>86</sub>	2S <sup>(0.96)</sup> 2p <sup>(3.14)</sup> 3p <sup>(0.01)</sup>	2S <sup>(0.95)</sup> 2p <sup>(3.11)</sup> 3p <sup>(0.02)</sup>	2S <sup>(0.96)</sup> 2p <sup>(3.14)</sup> 3p <sup>(0.01)</sup>	2S <sup>(0.95)</sup> 2p <sup>(3.11)</sup> 3p <sup>(0.02)</sup>

**Table 6.** The Natural Electron Configuration of some Atoms of the Ectoine before and after Reaction with Histidine Modified PAMAM in Gas and Solvent Phases

Atoms	Gas		Solvent	
	Before	After	Before	After
N <sub>52</sub>	2S(1.38)2p(4.51)	2S(1.36)2p(4.35)	2S(1.38)2p(4.53)	2S(1.36)2p(4.35)
H <sub>65</sub>	1S(0.60)	1S(0.62)	1S(0.60)	1S(0.60)
C <sub>50</sub>	2S(0.97)2p(3.15)	2S(0.94)2p(3.11)	2S(0.97)2p(3.15)	2S(0.95)2p(3.11)
O <sub>66</sub>	2S <sup>(1.71)</sup> 2p <sup>(4.84)</sup>	2S(1.74)2p(4.75)3p(0.01)	2S <sup>(1.70)</sup> 2p <sup>(4.91)</sup>	2S(1.73)2p(4.80)3p(0.01)
C <sub>67</sub>	2S <sup>(0.76)</sup> 2p <sup>(2.44)</sup>	2S(0.83)2p(2.46)	2S <sup>(0.77)</sup> 2p <sup>(2.41)</sup>	2S(0.83)2p(2.44)
C <sub>68</sub>	2S <sup>(0.96)</sup> 2p <sup>(3.14)</sup> 3p <sup>(0.01)</sup>	2S(0.95)2p(3.12)3p(0.01)	2S <sup>(0.96)</sup> 2p <sup>(3.14)</sup> 3p <sup>(0.01)</sup>	2S(0.95)2p(3.12)3p(0.01)

appropriate in bonding analysis applying Mulliken population analysis and semi-empirical calculation approaches. To show Ectoine-PAMAM and Ectoine-histidine modifies PAMAM bonds, the bond lengths, Fuzzy Bond Order, and Mayer Bond Order were calculated as listed in Tables 7 and 8. The bond length of key atoms in the solution phase increased slightly relative to the gas phase, and therefore the bond order decreased. The bond length of N43-C66 in the solution phase is shorter than the gas phase and a shorter bond length indicated a stronger bond. The amounts of MBO show that bond order reduced after the reaction in both phases. The amounts of FBO show that the bond order between the drug and the PAMAM dendrimer is the same in both phases. To indicate PAMAM-His-Ect bonds, the bond length of key atoms in the solution phase increased slightly relative to the gas phase, and therefore the bond order decreased. The amounts of MBO and FBO indicate that bond order reduced after reaction in

both phases.

The density of the states of a system is defined as the number of various states which are to be occupied by the system at every energy. DOS computations permit one to identify the general distribution of states as an energy function. DOS spectra help better understand the reaction between Ectoine-PAMAM and Ectoine-Histidine modified PAMAM. DOS computation showed that there is not much between Ectoine, PAMAM in the gas phase and water solvent. Therefore, the difference between HOMO and LUMO energies in two phases is little. DOS spectra Histidine modified PAMAM, the difference among energies gap in two phases is 0.11 eV, and this small difference is also observed in DOS spectra for Histidine modified PAMAM. After the reaction between ectoine and PAMAM (see Fig. 5), the difference between HOMO energies in two phases is 0.5 eV and also the value of 0.4 eV for LUMO energies. Therefore, this reaction causes that in the gas

**Table 7.** Bond Distance (Å), Mayer Bond Order (MBO), and Fuzzy Bond Order (FBO) some of Bonds of the Ectoine before and after Reaction with PAMAM in Gas and Solvent Phases

Bond	Bond length				MBO				FBO			
	Gas		Solvent		Gas		Solvent		Gas		Solvent	
	Before	After	Before	After	Before	After	Before	After	Before	After	Before	After
N <sub>43</sub> -H <sub>44</sub>	1.0000	1.0091	1.0139	1.0096	0.8685	0.7961	0.8632	0.7960	0.9024	0.7729	0.899	0.7729
O <sub>65</sub> -C <sub>66</sub>	1.2258	1.2517	1.2327	1.2619	1.9306	1.7703	1.8990	1.7703	1.9834	1.8253	1.9493	1.8253
N <sub>43</sub> -C <sub>66</sub>	-	1.3605	-	1.3509	-	1.0823	-	1.0825	-	1.4063	-	1.4063
C <sub>66</sub> -C <sub>67</sub>	1.5370	1.5378	1.5321	1.5377	0.7965	0.8082	0.7997	0.8081	0.9656	0.9691	0.9732	0.9692
C <sub>34</sub> -N <sub>43</sub>	1.4700	1.4604	1.4719	1.4621	0.9300	0.8453	0.9154	0.8453	1.2675	1.1406	1.2639	1.1406

**Table 8.** Bond Distance (Å), Mayer Bond Order (MBO), and Fuzzy Bond Order (FBO) some of Bonds of the Ectoine before and after Reaction with Histidine Modified PAMAM in Gas and Solvent Phases

Bond	Bond length				MBO				FBO			
	Gas		Solvent		Gas		Solvent		Gas		Solvent	
	Before	After	Before	After	Before	After	Before	After	Before	After	Before	After
N <sub>52</sub> -H <sub>65</sub>	1.0040	1.0075	1.0126	1.0077	0.8575	0.8383	0.8519	0.8118	0.8745	0.8179	0.8725	0.8104
O <sub>66</sub> -C <sub>67</sub>	1.2258	1.2474	1.2327	1.2559	1.9306	1.8885	1.8990	1.8101	1.9834	1.8737	1.9493	1.8274
N <sub>52</sub> -C <sub>67</sub>	-	1.3747	-	1.3614	-	0.9435	-	0.9952	-	1.3146	-	1.3666
C <sub>67</sub> -C <sub>68</sub>	1.5370	1.5411	1.5321	1.5401	0.7965	0.7785	0.7997	0.7868	0.9656	0.9621	0.9732	0.9577
C <sub>50</sub> -N <sub>52</sub>	1.4671	1.4637	1.4761	1.4630	0.9598	0.8957	0.9338	0.8647	1.1982	1.1100	1.1965	1.1083

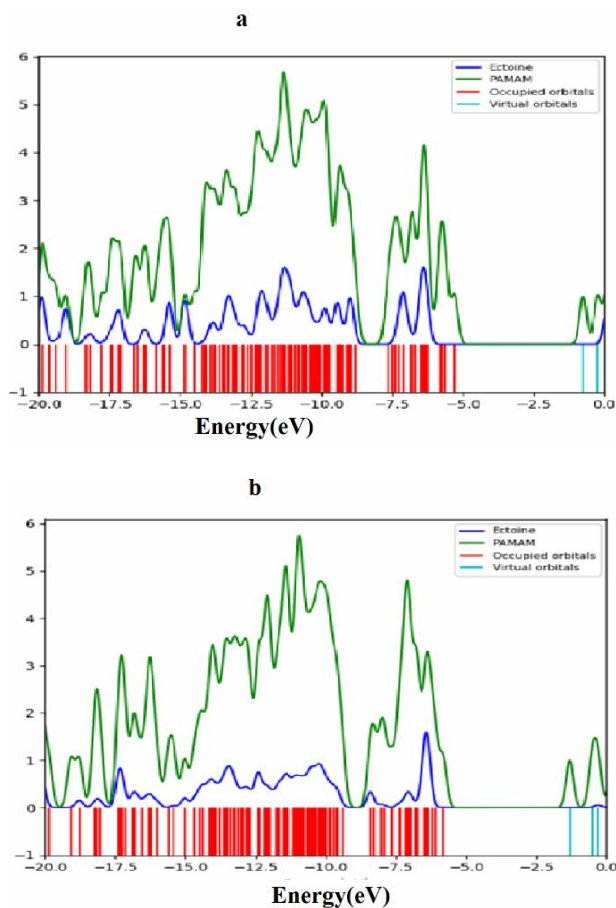


**Fig. 5.** DOS plots of optimized Ectoine-PAMAM a) at gas and b) at solvent phases.

phase the HOMO level shifts to lower energy compared to the solvent phase, while the LUMO level is almost unchanged. After the reaction between ectoine and Histidine modified PAMAM (see Fig. 6), there is not any difference between HOMO energies in two phases, the difference among LUMO energies in two phases is 0.07 eV.

## CONCLUSIONS

DFT computations were done to investigate the reaction of PAMAM and Histidine modified PAMAM dendrimers with Ectoine anticancer drug. In this article, the bond of dendrimers and Ectoine drug was made by an EDC/NHS cross-linking. Our results show that both PAMAM-Ectoine and Histidine modified PAMAM-Ectoine complexes can

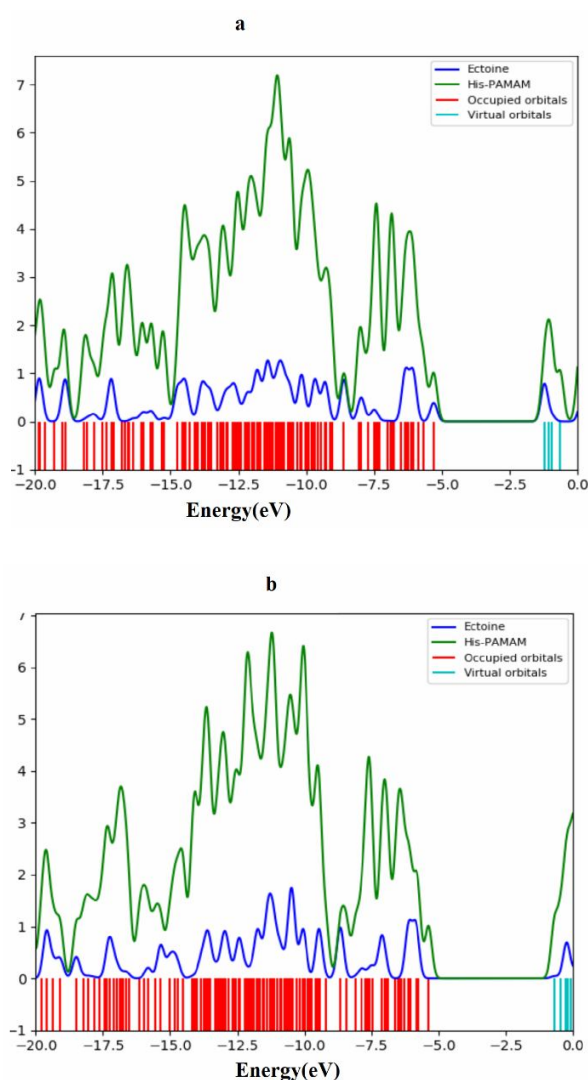


**Fig. 6.** DOS plots of optimized Ectoine-Histidine modified PAMAM a) at gas and b) at solvent phases.

adsorb more electrons in the water solvent. As well, the characteristics of bonding between Ectoine and dendrimers are covalent. Moreover, the bonding of Histidine modified PAMAM-Ectoine complex is more covalent than PAMAM-Ectoine. The binding energy of PAMAM-Ectoine showed that this energy reduces from -31.085 eV in the gas phase to -65.834 eV in the solvent phase. For Histidine modified PAMAM-Ectoine, the binding energy from -39.584 to -95.934 eV was reduced. Also, the computations of NBO analysis, bond lengths and Mayer bond order, and Fuzzy

bond order analysis of compounds were done to approve the covalent bond. DOS spectra of Ectoine-dendrimers complexes are similar to the trends of their energy gaps in two phases.

## ACKNOWLEDGMENTS

The authors are grateful to the Payame Noor University for encouragement.

## REFERENCES

- [1] Marasini, N.; Haque, S.; Kaminskas, L. M., Polymer-drug conjugates as inhalable drug delivery systems: a review. *Curr. Opin. Colloid Interface Sci.* **2017**, *31*, 18-29. DOI: 10.1016/j.cocis.2017.06.003.
- [2] Pattni, B. S.; Chupin, V. V.; Torchilin, V. P., New developments in liposomal drug delivery. *Chem. Rev.* **2015**, *115*, 10938-10966. DOI: 10.1021/acs.chemrev.5b00046.
- [3] Raza, K.; Thotakura, N.; Kumar, P.; Joshi, M.; Bhushan, S.; Bhatia, A.; Kumar, V.; Malik, R.; Sharma, G.; Guru, S. K., C60-fullerenes for delivery of docetaxel to breast cancer cells: a promising approach for enhanced efficacy and better pharmacokinetic profile. *Int. J. Pharmaceut.* **2015**, *495*, 551-559. DOI: 10.1016/j.ijpharm.2015.09.016.
- [4] Naiafi, M., Antioxidant activity of sesamol derivatives and their drug delivery via C60 nanocage: a theoretical study. *Chin. J. Struct. Chem.* **2019**, *38*, 195-200. DOI: 10.14102/j.cnki.0254-5861.2011-2113.
- [5] Spencer, D. S.; Puranik, A. S.; Peppas, N. A., Intelligent nanoparticles for advanced drug delivery in cancer treatment. *Curr. Opin. Chem. Eng.* **2015**, *7* 84-92. DOI: 10.1016/j.coche.2014.12.003.
- [6] Khorram, R.; Morsali, A.; Raissi, H.; Hakimi, M.; Beyramabadi, S.A. Mechanistic, energetic and structural aspects of the adsorption of carmustine on the functionalized carbon nanotubes. *Chin. J. Struct. Chem.* **2017**, *36*, 1639-1646. DOI: 10.14102/j.cnki.0254-5861.2011-1588.
- [7] Kamel, M.; Raissi, H.; Morsali, A.; Shahabi, M., Assessment of the adsorption mechanism of flutamide anticancer drug on the functionalized single-walled carbon nanotube surface as a drug delivery vehicle: An alternative theoretical approach based on DFT and MD. *App. Sur. Sci.* **2018** *434*, 492-503. DOI: 10.1016/j.apsusc.2017.10.165.
- [8] Kabanov, A., Biomedical applications of nano-sized polymeric micelles and polyion complexes. *J. Sib. Fed. Univ. Biol.* **2018**, *11*, 110-118. DOI:10.17516/1997-1389-0053.
- [9] Singh, I.; Rehni, A.; Kalra, R.; Joshi, G.; Kumar, M., Dendrimers and their pharmaceutical applications-a review. *Die Pharmazie: Int. J. Pharmaceut. Sci.* **2008**, *63*, 491-496. DOI: 10.1691/ph.2008.8052.
- [10] Svenson, S.; Tomalia, D. A., Dendrimers in biomedical applications-reflections on the field. *Adv. Drug Deliv. Rev.* **2012**, *64*, 102-115. DOI: 10.1016/j.addr.2012.09.030.
- [11] Gupta, A.; Dubey, S.; Mishra, M., Unique structures, properties and applications of dendrimers. *J. Drug Del. Ther.* **2018**, *8*, 328-339. DOI: 10.22270/jddt.v8i6-s.2083.
- [12] Du, L.; Jin, Y.; Yang, J.; Wang, S.; Wang, X., A functionalized poly (amidoamine) nanocarrier loading 5-fluorouracil: pH-responsive drug release and enhanced anticancer effect. *Anti-cancer drugs.* **2013**, *24*, 172-180. DOI: 10.1097/CAD.0b013e32835920fa.
- [13] Yellepeddi, V. K.; Kumar, A.; Maher, D. M.; Chauhan, S. C.; Vangara, K. K.; Palakurthi, S., Biotinylated PAMAM dendrimers for intracellular delivery of cisplatin to ovarian cancer: role of SMVT. *Anticancer Res.* **2011**, *31*, 897-906.
- [14] Zhu, S.; Hong, M.; Zhang, L.; Tang, G.; Jiang, Y.; Pei, Y., PEGylated PAMAM dendrimer doxorubicin conjugates: *in vitro* evaluation and *in vivo* tumor accumulation. *Pharmaceut. Res.* **2010**, *27*, 161-174. DOI: 10.1007/s11095-009-9992-1
- [15] Xie, Y.; Yao, Y., Incorporation with dendrimer-like biopolymer leads to improved soluble amount and *in vitro* anticancer efficacy of paclitaxel. *J. Pharmaceut. Sci.* **2019**, *108*, 1984-1990. DOI: 10.1016/j.xphs.2018.12.026.
- [16] Morgan, M. T.; Carnahan, M. A.; Immoos, C. E.; Ribeiro, A. A.; Finkelstein, S.; Lee, S. J.; Grinstaff, M. W., Dendritic molecular capsules for hydrophobic compounds. *J. Am. Chem. Soc.* **2003**, *125*, 15485-

15489. DOI: 10.1021/ja0347383.
- [17] Scutaru, A. M.; Wenzel, M.; Scheffler, H.; Wolber, G.; Gust, R., Optimization of the N-lost drugs melphalan and bendamustine: synthesis and cytotoxicity of a new set of dendrimer-drug conjugates as tumor therapeutic agents. *Bioconjug. Chem.* **2010**, *21*, 1728-1743. DOI: 10.1021/bc900406m.
- [18] Zhang, X.; Zeng, Y.; Yu, T.; Chen, J.; Yang, G.; Li, Y., Tetrathiafulvalene terminal-decorated PAMAM dendrimers for triggered release synergistically stimulated by redox and CB. *Langmuir* **2014**, *30*, 718-726. DOI: 10.1021/la404349w.
- [19] Aulenta, F.; Hayes, W.; Rannard, S., Dendrimers: a new class of nanoscopic containers and delivery devices. *Eur. Pol. J.* **2003**, *39*, 1741-1771. DOI: 10.1016/S0014-3057(03)00100-9.
- [20] Wu, S. Y.; Chou, H. Y.; Tsai, H. C.; Anbazhagan, R.; Yuh, C. -H.; Yang, J. M.; Chang, Y. H., Amino acid-modified PAMAM dendritic nanocarriers as effective chemotherapeutic drug vehicles in cancer treatment: a study using zebrafish as a cancer model. *RSC Adv.* **2020**, *10*, 20682-20690. DOI: 10.1039/D0RA01589J.
- [21] Emanuele, A. D.; Attwood, D., Dendrimer-drug interactions. *Adv. Drug Deliv. Rev.* **2005**, *57*, 2147-2162. DOI: 10.1016/j.addr.2005.09.012.
- [22] Sheikhpour, M.; Sadeghi, A.; Yazdian, F.; Movafagh, A.; Mansoori, A., Anticancer and apoptotic effects of ectoine and hydroxyectoine on non-small cell lung cancer cells: An in-vitro investigation. *Multidiscipl. Cancer Invest.* **2019**, *3*, 14-20. DOI: 10.30699/acadpub.mci.3.2.14.
- [23] Pastor, J.M.; Salvador, M.; Argandona, M.; Bernal, V.; Reina-Bueno, M.; Csonka, L. N.; Iborra, J. L.; Vargas, C.; Nieto, J. J.; Canovas, M., Ectoines in cell stress protection: Uses and biotechnological production. *Biotechnol. Adv.* **2010**, *28*, 782-801. DOI: 10.1016/j.biotechadv.2010.06.005
- [24] Hahn, M. B.; Meyer, S.; Schroter, M. A.; Kunte, H. J.; Solomun, T.; Sturm, H., DNA protection by ectoine from ionizing radiation Molecular mechanisms. *Phys. Chem. Chem. Phys.* **2017**, *19*, 25717-25722. DOI: 10.1039/C7CP02860A.
- [25] Wells, L. A.; Furukawa, S.; Sheardown, H.; Wells, L. A.; Furukawa, S.; Sheardown, H., Photoresponsive PEG-anthracene grafted hyaluronan as a controlled-delivery biomaterial. *Biomacromolecules* **2011**, *12*, 923-932. DOI: 10.1021/bm101233m.
- [26] Phelps, J. A.; Morisse, S.; Hindie, M.; Degat, M. C.; Pauthe, E.; Van Tassel, P. R., Nanofilm biomaterials: localized cross-linking to optimize mechanical Rigidity and bioactivity, *Langmuir* **2011**, *27*, 1123-1130. DOI: 10.1021/la104156c.
- [27] Sam, S.; Touahir, L.; Andresa, J. S.; Allongue, P.; Chazalviel, J. N.; Gouget-Laemmel, A. C.; Villeneuve, C. H.; Moraillon, A.; Ozanam, F.; Gabouze, N.; Djebba, S., Semiquantitative study of the EDC/NHS activation of acid terminal groups at modified porous silicon surfaces. *Langmuir* **2010**, *26*, 809-814. DOI: 10.1021/la902220a.
- [28] Haghghi, F.; Morsali, A.; Bozorgmehra, M. R.; Beyramabadi, S. A., Nanostructures of PAMAM dendrimers in drug delivery system for 5-fluorouracil. *J. Sib. Fed. Univ. Chem.* **2020**, *13*, 309-323. DOI: 10.17516/1998-2836-0184.
- [29] Bayat, M.; Taherpour, A. A.; Elahi, S. M., Molecular interactions between PAMAM dendrimer and some medicines that suppress the growth of hepatitis virus (Adefovir, Entecavir, Telbivudine, Lamivudine, Tenofovir): a theoretical study. *Int. Nano Lett.* **2019**, *9*, 231-244. DOI: 10.1007/s40089-019-0277-3.
- [30] Farmanzadeh, D.; Ghaderi, M., A computational study of PAMAM dendrimer interaction with *trans* isomer of picoplatin anticancer drug. *J. Mol. Graph. Model.* **2018**, *80*, 1-6. DOI:10.1016/j.jmkgm.2017.12.010.
- [31] Ehsani, E.; Shojaie, F., DFT computational investigation of the reaction behavior of polyamidoamine dendrimer as nanocarrier for delivery of melphalan anticancer drug. *J. Mol. Liq.* **2021**, *323*, 114625-114639. DOI: 10.1016/j.molliq.2020.114625.
- [32] Camarada, M. DFT investigation of the interaction of gold nanoclusters with poly (amidoamine) PAMAM G0 dendrimer. *Chem. Phys. Lett.* **2016**, *654*, 29-36. DOI: 10.1016/j.cplett.2016.05.007.
- [33] Vergara-Jaque, A.; Comer, J.; Monsalve, L.; González-Nilo, F.D.; Sandoval, C. Computationally efficient methodology: a comparison of amine-and acetyl-terminated PAMAM, *J. Phys. Chem. B* **2013**, *117*, 6801-6813. DOI: 10.1021/jp4000363.

- [34] Pooja, D.; Kulhari, H.; Singh, M. K.; Mukherjee, S.; Rachamalla, S. S.; Sistla, R., Dendrimer-TPGS mixed micelles for enhanced solubility and cellular toxicity of taxanes, *Colloids Surf. B Biointerfaces* **2014**, *121*, 461-468. DOI: 10.1016/j.colsurfb.2014.06.059.
- [35] Katare, Y. K.; Daya, R. P.; Sookram Gray, C.; Luckham, R. E.; Bhandari, J.; Chauhan, A. S.; Mishra, R. K., Brain targeting of a water insoluble antipsychotic drug haloperidol *via* the intranasal route using PAMAM dendrimer, *Mol. Pharm.* **2015**, *12*, 3380-3388. DOI: 10.1021/acs.molpharmaceut.5b00402.
- [36] Badalkhani-Khamseh, F.; Bahrami, A.; Ebrahim-Habibi, A.; Hadipour, N. L., Complexation of nicotinic acid with first generation poly (amidoamine) dendrimers: a microscopic view from density functional theory, *Chem. Phys. Lett.* **2017**, *684*, 103-112. DOI: 10.1016/j.cplett.2017.06.042.
- [37] Soto-Castro, D.; Evangelista-Lara, A.; Guadarrama, P., Theoretical design of dendrimeric fractal patterns for the encapsulation of a family of drugs: salicylanilides, *Tetrahedron* **2006**, *62*, 12116-12125. DOI: 10.1016/j.tet.2006.08.053.
- [38] Ramos, M. C.; Horta, B. A. C., Drug-loading capacity of PAMAM dendrimers encapsulating quercetin molecules: a molecular dynamics study with the 2016H66 force field. *J. Chem. Inf. Mod.* **2021**, *22*, 987-1000. DOI: 10.1021/acs.jcim.0c00960.
- [39] Frisch, M.; Trucks, G.; Schlegel, H.; Scuseria, G.; Robb, M.; Cheeseman, J.; Scalmani, G.; Barone, V.; Mennucci, B.; Petersson, G., Gaussian 09, Revision A.02, Gaussian, Inc., Wallingford, CT, **2009**.
- [40] Lopez, N.; Illas, F., *Ab initio* modeling of the metal-support interface: The interaction of Ni, Pd, and Pt on MgO (100). *J. Phys. Chem. B* **1998**, *102*, 1430-1436. DOI: 10.1021/jp972626q.
- [41] Lu, T.; Chen, F., Multiwfn: a multifunctional wavefunction analyzer. *J. Comput. Chem.* **2012**, *33*, 580-592. DOI: 10.1002/jcc.22885.
- [42] Mayer, I.; Salvador, P., Overlap populations, bond orders and valences for fuzzy atoms. *Chem. Phys. Lett.* **2004**, *383*, 368-375. DOI: 10.1016/j.cplett.2003.11.048
- [43] Mayer, I., Charge, bond order and valence in the *Ab initio* SCF theory. *Chem. Phys. Lett.* **1983**, *97*, 270-274. DOI: 10.1016/0009-2614(83)80005-0.
- [44] Lu, T.; Chen, F. W., Meaning and functional form of the electron localization function. *Acta Phys.-Chim. Sin.* **2011**, *27*, 2786-2792. DOI: 10.3866/PKU.WHXB20112786.
- [45] Lipparini, F.; Scalmani, G.; Mennucci, B.; Frisch, M. J., Self-consistent field and polarizable continuum model: a new strategy of solution for the coupled equations. *J. Chem. Theory Comput.* **2011**, *7*, 610-617. DOI: 10.1021/ct1005906.
- [46] Bankiewicz, B.; Matczak, P.; Palusiak, M. Electron density characteristics in bond critical point (QTAIM) versus interaction energy components (SAPT). *J. Phys. Chem. A* **2011**, *116*, 452-459. DOI: 10.1021/jp210940b.
- [47] Jacobsen, H.; Jacobsen, H., Chemical bonding in view of electron charge density and kinetic energy density descriptors. *J. Comput. Chem.* **2009**, *30*, 1093-1102. DOI: 10.1002/jcc.21135.
- [48] Becke, A. D.; Edgecombe, K. E., A simple measure of electron localization in atomic and molecular systems. *J. Chem. Phys.* **1990**, *92*, 5397-5401. DOI: 10.1063/1.458517.
- [49] Fuentealba, P.; Chamorro, E.; Santos, J. C., Chapter 5 understanding and using the electron localization function. *Theor. Comput. Chem.* **2007**, *19*, 57-85. DOI: 10.1016/S1380-7323(07)80006-9.